

1-1-2015

Ultra-low viscosity liquid crystal materials

Haiwei Chen
University of Central Florida

Minggang Hu
University of Central Florida

Fenglin Peng
University of Central Florida

Jian Li

Zhongwei An

See next page for additional authors

Find similar works at: <https://stars.library.ucf.edu/facultybib2010>
University of Central Florida Libraries <http://library.ucf.edu>

This Article is brought to you for free and open access by the Faculty Bibliography at STARS. It has been accepted for inclusion in Faculty Bibliography 2010s by an authorized administrator of STARS. For more information, please contact STARS@ucf.edu.

Recommended Citation

Chen, Haiwei; Hu, Minggang; Peng, Fenglin; Li, Jian; An, Zhongwei; and Wu, Shin-Tson, "Ultra-low viscosity liquid crystal materials" (2015). *Faculty Bibliography 2010s*. 6460.
<https://stars.library.ucf.edu/facultybib2010/6460>

Authors

Haiwei Chen, Minggang Hu, Fenglin Peng, Jian Li, Zhongwei An, and Shin-Tson Wu

Ultra-low viscosity liquid crystal materials

Haiwei Chen,¹ Minggang Hu,^{1,2} Fenglin Peng,¹ Jian Li,² Zhongwei An,²
and Shin-Tson Wu^{1,*}

¹CREOL, The College of Optics and Photonics, University of Central Florida, Orlando, FL 32816, USA

²Xi'an Modern Chemistry Research Institute, Xi'an 710065, China

*swu@ucf.edu

Abstract: We report five ultra-low viscosity nematic liquid crystal mixtures with birefringence around 0.1, dielectric anisotropy in the range of 3 to 6, and clearing temperature about 80°C. A big advantage of these low viscosity mixtures is low activation energy, which significantly suppresses the rising rate of viscosity at low temperatures. Using our mixture M3 as an example, the response time of a 3- μm cell at -20°C is only 30 ms. Widespread application of these materials for display devices demanding a fast response time, especially at low temperatures, is foreseeable.

©2015 Optical Society of America

OCIS codes: (160.3710) Liquid crystals; (230.3720) Liquid-crystal devices.

References and links

1. M. Schadt, "Milestone in the history of field-effect liquid crystal displays and materials," *Jpn. J. Appl. Phys.* **48**, 03B001 (2009).
2. K.-H. Fan-Chiang, C.-C. Lai, J.-T. Cheng, C.-C. Yen, B.-J. Liao, Y.-Y. Ho, and Y.-C. Chen, "P-173: A 0.38" field-sequential-color liquid-crystal-on-silicon microdisplay for mobile projectors," *Dig. Tech. Pap.* **40**(1), 1770–1773 (2009).
3. Z. Luo, F. Peng, H. Chen, M. Hu, J. Li, Z. An, and S. T. Wu, "Fast-response liquid crystals for high image quality wearable displays," *Opt. Mater. Express* **5**(3), 603–610 (2015).
4. Y. Iwata, M. Murata, K. Tanaka, T. Ohtake, H. Yoshida, and K. Miyachi, "Novel super fast response vertical alignment-liquid crystal display with extremely wide temperature range," *J. Soc. Inf. Disp.* **22**(1), 35–42 (2014).
5. S. J. Kim, H. Y. Kim, S. H. Lee, Y. K. Lee, K. C. Park, and J. Jang, "Cell gap-dependent transmittance characteristic in a fringe field-driven homogeneously aligned liquid crystal cell with positive dielectric anisotropy," *Jpn. J. Appl. Phys.* **44**(9A), 6581–6586 (2005).
6. S. H. Lee, S. L. Lee, and H. Y. Kim, "Electro-optic characteristics and switching principle of a nematic liquid crystal cell controlled by fringe-field switching," *Appl. Phys. Lett.* **73**(20), 2881–2883 (1998).
7. Z. Ge, S. T. Wu, S. S. Kim, J. W. Park, and S. H. Lee, "Thin cell fringe-field-switching liquid crystal display with a chiral dopant," *Appl. Phys. Lett.* **92**(18), 181109 (2008).
8. J. Li, C. H. Wen, S. Gauza, R. Lu, and S. T. Wu, "Refractive indices of liquid crystals for display applications," *J. Display Technol.* **1**(1), 51–61 (2005).
9. H. Takatsu, "Advanced liquid crystal materials for active matrix displays," *Conf. Proc. Advanced Display Materials and Devices*, p.43 (Sendai, Japan, 2014).
10. J. Li, M. Hu, J. Li, Z. An, X. Yang, Z. Yang, and Z. Che, "Highly fluorinated liquid crystals with wide nematic phase interval and good solubility," *Liq. Cryst.* **41**(12), 1783–1790 (2014).
11. M. Schadt, R. Buchecker, and K. Muller, "Material properties, structural relations with molecular ensembles and electro-optical performance of new bicyclohexane liquid crystals in field-effect liquid crystal displays," *Liq. Cryst.* **5**(1), 293–312 (1989).
12. J. W. Ryu, J. Y. Lee, H. Y. Kim, J. W. Park, G. D. Lee, and S. H. Lee, "Effect of magnitude of dielectric anisotropy of a liquid crystal on light efficiency in the fringe-field switching nematic liquid crystal cell," *Liq. Cryst.* **35**(4), 407–411 (2008).
13. S. T. Wu and C. S. Wu, "Experimental confirmation of the Osipov-Terentjev theory on the viscosity of nematic liquid crystals," *Phys. Rev. A* **42**(4), 2219–2227 (1990).
14. S. W. Kang, I. W. Jang, D. H. Kim, Y. J. Lim, and S. H. Lee, "Enhancing transmittance of fringe-field switching liquid crystal device by controlling perpendicular component of dielectric constant of liquid crystal," *Jpn. J. Appl. Phys.* **53**(1), 010304 (2014).
15. H. Chen, F. Peng, Z. Luo, D. Xu, S. T. Wu, M. C. Li, S. L. Lee, and W. C. Tsai, "High performance liquid crystal displays with a low dielectric constant material," *Opt. Mater. Express* **4**(11), 2262–2273 (2014).
16. S. T. Wu, "Birefringence dispersions of liquid crystals," *Phys. Rev. A* **33**(2), 1270–1274 (1986).
17. S. T. Wu, U. Efron, and L. D. Hess, "Birefringence measurements of liquid crystals," *Appl. Opt.* **23**(21), 3911–3915 (1984).

18. I. Haller, "Thermodynamic and static properties of liquid crystals," *Prog. Solid State Chem.* **10**(2), 103–118 (1975).
 19. M. Oh-e and K. Kondo, "Electro-optical characteristics and switching behavior of the in-plane switching mode," *Appl. Phys. Lett.* **67**(26), 3895–3897 (1995).
 20. Y. Chen, F. Peng, T. Yamaguchi, X. Song, and S. T. Wu, "High performance negative dielectric anisotropy liquid crystals for display applications," *Crystals* **3**(3), 483–503 (2013).
 21. L. M. Blinov and V. G. Chigrinov, *Electrooptic Effects in Liquid Crystal Materials* (Springer-Verlag, 1994).
 22. S. T. Wu and C. S. Wu, "Rotational viscosity of nematic liquid crystals A critical examination of existing models," *Liq. Cryst.* **8**(2), 171–182 (1990).
 23. W. H. De Jeu, "Physical properties of liquid crystalline materials in relation to their applications," *Mol. Cryst. Liq. Cryst. (Phila. Pa.)* **63**(1), 83–109 (1981).
 24. L. Rao, S. Gauza, and S. T. Wu, "Low temperature effects on the response time of liquid crystal displays," *Appl. Phys. Lett.* **94**(7), 071112 (2009).
-

1. Introduction

Fast response time is one of the most critical requirements for most liquid crystal display (LCD) devices [1] because it helps reduce motion picture image blur and crosstalk, enhance optical efficiency, and suppress color mixing for field-sequential displays [2, 3]. Mobile displays, wearable displays, and car navigation systems are often used in outdoor and they have to endure harsh weather conditions, like low temperatures (-20°C). In such a cold ambient temperature, LC response time is usually as sluggish as several hundreds of milliseconds. As a result, the displayed image quality is severely degraded [4].

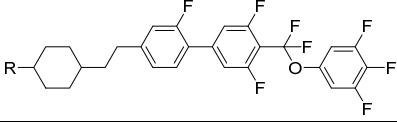
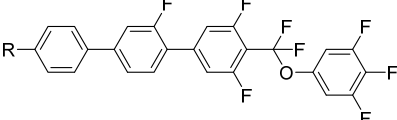
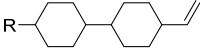
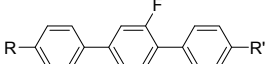
To shorten response time, a straightforward approach is to decrease the LC cell gap (d). However, for an LCD a certain $d\Delta n$ value is required in order to obtain high transmittance; here Δn is the LC birefringence. For example, the commonly used fringe field switching (FFS) LCD requires $d\Delta n \approx 320\text{--}340$ nm in order to achieve high transmittance [5, 6]. Although thin cell gap helps greatly to achieve fast response time [7], this approach imposes two problems: it reduces manufacturing yield and it demands a higher Δn LC, which has stronger wavelength dispersion [8]. To obtain white color, the transmittance of red, green, and blue sub-pixels should be balanced. From experimental studies, the preferred Δn for FFS is around 0.10 ± 0.01 . Under such circumstance, the cell gap is about $3\ \mu\text{m}$, which is still manageable for high-yield manufacturing. With abovementioned constraints, the simplest way to reduce response time is to employ a low viscosity LC.

In this paper, we formulated five ultra-low viscosity LC mixtures with $\Delta n \approx 0.1$, dielectric anisotropy $\Delta\epsilon \approx 3$ to 6, and clearing temperature about 80°C . A big advantage of these low viscosity LC mixtures is their small activation energy, which significantly suppresses the rising rate of viscosity at low temperatures. Using our mixture M3 as an example, the response time of a $3\text{-}\mu\text{m}$ FFS cell at -20°C is about 30ms. These materials will find widespread applications for display devices that demand a fast response time.

2. Mixture formulation

Our low viscosity LC mixtures contain three major ingredients: 1) high Δn and large $\Delta\epsilon$ compounds, 2) ultra-low viscosity diluters, and 3) wide nematic range compounds. Table 1 lists the chemical structures and compositions of our five mixtures. Compounds 1 and 2 have high Δn and large $\Delta\epsilon$ (>25) [9, 10], but their viscosity is also high. To lower the viscosity, we added more than 40% non-polar diluters (#3) [11]. To widen nematic range and achieve high clearing point, we added some terphenyl compounds (#4). To obtain different $\Delta\epsilon$ values, we formulated five LC mixtures by varying the compound concentrations as Table 1 shows.

Table 1. Chemical structures and compositions of LC mixtures; R and R' represent alkyl chains.

No.	Compound Structure	Mixtures (wt%)				
		M1	M2	M3	M4	M5
1		12%	11%	12%	13%	24%
2		10%	12%	13%	18%	18%
3		56%	55%	53%	48%	40%
4		22%	22%	22%	21%	18%

3. Material characterization

In experiment, we measured the dielectric anisotropy, birefringence, visco-elastic constant, and activation energy of these five mixtures. To avoid crowdedness of data presentation, here we only show the measured results of M3, M4, and M5 in the following Sections. Table 2 summarizes the key results of these five mixtures.

3.1 Dielectric anisotropy

Dielectric anisotropy affects the operation voltage, peak transmittance [12], and response time (through viscosity) of the FFS LCD. To reduce the power consumption of a mobile display, it is desirable to keep the on-state voltage below 5V. This requirement demands a fairly large $\Delta\epsilon$. On the other hand, to obtain low viscosity we should keep $\Delta\epsilon$ as small as possible. Thus, there exist contradicting requirements for $\Delta\epsilon$ between low operation voltage and fast response time. A compromised $\Delta\epsilon$ value is in the range of 3 to 6.

Table 2. Measured properties of the five LC mixtures at $T = 23^\circ\text{C}$, $\lambda = 633\text{nm}$, and $f = 1$ kHz.

	$\epsilon_{//}$	ϵ_{\perp}	$\Delta\epsilon$	Δn	K_{11} (pN)	γ_l (mPas)	γ_l/K_{11}	T_c ($^\circ\text{C}$)	E (meV)
M1	5.66	2.61	3.05	0.098	11.8	41.3	3.50	78.8	190
M2	5.91	2.68	3.23	0.102	12.2	42.2	3.46	79.5	195
M3	6.26	2.76	3.50	0.100	11.7	45.1	3.85	77.9	205
M4	7.43	2.83	4.60	0.097	12.1	50.4	4.17	80.1	228
M5	9.51	3.33	6.18	0.099	11.4	53.3	4.68	75.5	260

In experiment, we used the capacitance method to measure the dielectric constants ($\epsilon_{//}$ and ϵ_{\perp}) of our five LC mixtures at room temperature (23°C). Detailed procedures have been reported in Ref [13], and the measured results are listed in Table 2. From Table 2, the $\epsilon_{//}$ and ϵ_{\perp} of M3 is 6.26 and 2.76, respectively, i.e., $\Delta\epsilon = 3.50$, which is much lower than that used in conventional p-FFS LCD ($\Delta\epsilon = 8\sim 10$) [14]. With such a low $\Delta\epsilon$, the operation voltage, which

is inversely proportional to the square root of $\Delta\epsilon$, would undoubtedly increase [12]. Fortunately, the transmittance of p-FFS increases as $\Delta\epsilon$ gradually decreases. As a result, we can still get high transmittance at a relatively low voltage (5V) using a low $\Delta\epsilon$ LC material [15]. For M4 and M5, the $\Delta\epsilon$ value is 4.60 and 6.18, respectively. Among these three mixtures studied, M3 contains the largest amount of diluters, thus its viscosity is the lowest but its dielectric anisotropy is also the smallest.

3.2 Temperature dependent birefringence

Birefringence of an LC is mainly governed by the conjugation length and order parameter [16]. To measure Δn , we filled the LC mixture into a homogeneous cell made of indium tin oxide (ITO) glass substrates. The inner surface of the ITO-glass was over-coated with a thin polyimide alignment layer. The pretilt angle was about 2° . The cell was sandwiched between two crossed linear polarizers. By measuring the voltage dependent transmittance through LabView system, we can obtain Δn easily. Detailed method has been described in [17]. From Table 2, the measured birefringence at room temperature is $\Delta n = 0.100$ for M3, 0.097 for M4, and 0.099 for M5. These values are very close to our ideal one, which is 0.1.

Next, we measured the temperature dependent birefringence. We placed the LC cell on a Linkam heating stage controlled by the temperature program (Linkam TMS94). Results are shown in Fig. 1, where dots stand for measured data and solid lines for the fittings using Haller's semi-empirical equation [18]:

$$\Delta n(T) = \Delta n_0 S = \Delta n_0 (1 - T / T_c)^\beta, \quad (1)$$

where Δn_0 is the extrapolated birefringence at $T = 0$, S is the order parameter, T is the temperature, T_c is the clearing point, and β is a material parameter. Through fittings, we found $\Delta n_0 = 0.138$ and $\beta = 0.174$ for M3, $\Delta n_0 = 0.133$ and $\beta = 0.177$ for M4, and $\Delta n_0 = 0.135$ and $\beta = 0.165$ for M5, respectively. Using these fitting parameters, we can calculate the order parameter (S), which will be used later.

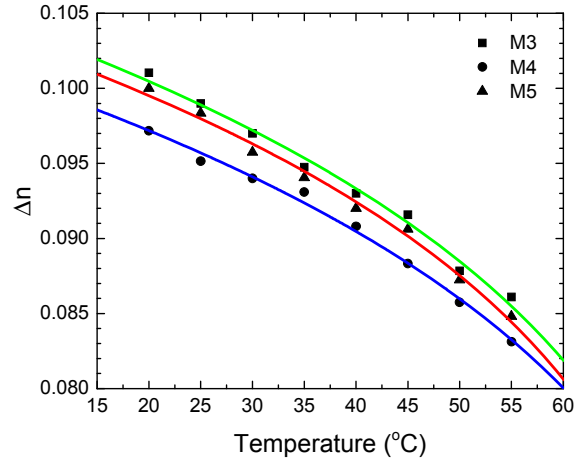


Fig. 1. Temperature dependent birefringence of M3, M4, and M5 at $\lambda = 633\text{nm}$. Dots are experimental data and solid lines are fitting curves with Eq. (1).

3.3 Elastic constant and viscosity

In an LCD, the response time is proportional to the visco-elastic coefficient (γ_1/K_{ii}), where K_{ii} is the corresponding elastic constant depending on the LC alignment. For examples, for vertical alignment, $K_{ii} = K_{33}$ is the bend elastic constant, and for in-plane switching (IPS) cell [19] $K_{ii} = K_{22}$ is the twist elastic constant. However for FFS, the electric field has transversal and longitudinal components so that both K_{22} and K_{11} are involved, although twist dominates

[20]. Several approaches have been proposed to measure γ_l and K_{11} . Here, we used the time dependent transmittance method described in Ref [13].

For a homogeneous cell, the threshold voltage is related to K_{11} and $\Delta\epsilon$ as [21]:

$$V_{th} = \pi\sqrt{K_{11}/(\epsilon_0 \cdot \Delta\epsilon)}, \quad (2)$$

where K_{11} is the splay elastic constant and ϵ_0 is the permittivity of vacuum. From the measured threshold voltage and dielectric anisotropy, we can extract K_{11} from Eq. (2). As listed in Table 2, all the five mixture we prepared have a very similar K_{11} value ($\sim 12\text{pN}$) because they basically consist of same compounds except at different compositions.

Next, we used the same setup as described in Sec. 3.2 to measure γ_l/K_{11} . Detailed method has been described in [13]. Since K_{11} has already been obtained from Eq. (2), we can extract γ_l from the measured γ_l/K_{11} . The measured γ_l is 45.1 mPas, 50.4 mPas, and 52.3 mPas for M3, M4, and M5, respectively. These γ_l values seem to correlate with $\Delta\epsilon$ linearly, as will be examined in more detail later.

3.4 Activation energy

As the temperature decreases, rotational viscosity increases exponentially as [22, 23]:

$$\gamma_l \sim S \cdot \exp(E/k_B T), \quad (3)$$

where E is the activation energy and k_B is the Boltzmann constant. From Eq. (3), activation energy determines the rising rate of rotational viscosity in the low temperature region. Key parameters affecting E include molecular structure and conformation, and intermolecular interactions [13]. As Table 1 shows, the low $\Delta\epsilon$ LC mixture contains more non-polar diluters. As a result, its activation energy is relatively small, which in turn only causes a mild increase as the temperature decreases. To extract E , we measured the temperature dependent viscoelastic coefficient of these mixtures using the same method discussed above. In theory, temperature dependent γ_l/K_{11} (homogenous cell) can be described as follows [22]:

$$K_{11} \sim S^2, \quad (4)$$

$$\gamma_l/K_{11} = A \cdot \exp(E/k_B T) / S. \quad (5)$$

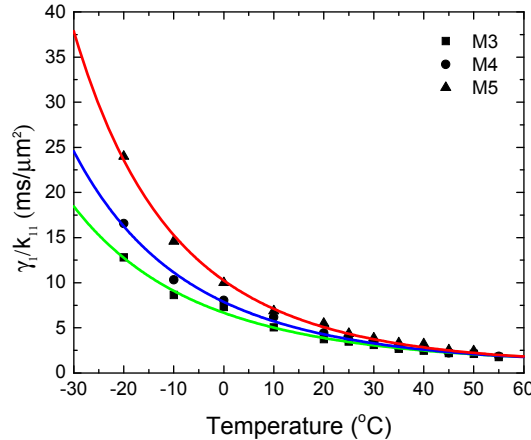


Fig. 2. Temperature dependent γ_l/K_{11} of M3, M4, and M5. Dots are experimental data and solid lines are fittings with Eq. (5).

Figure 2 depicts the measured data (dots) and fitted curves (solid lines). The measured data fit well with Eq. (5). Through fittings, we found $E = 205$ meV for M3, 228 meV for M4, and 260 meV for M5. For comparison, the reported activation energy of MLC-6686 ($\Delta\epsilon = 10$)

is 353.9 meV and MLC-6608 ($\Delta\varepsilon = -4.2$) is 496.0 meV [15, 24]. Our low viscosity LC mixtures exhibit much lower activation energy. In experiment, we tested a 3.5- μm FFS cell with electrode width $l = 3\mu\text{m}$, electrode gap $g = 4\mu\text{m}$ using M3. Peak transmittance (90.4%) was achieved at 7.1 V_{rms} under $\lambda = 514\text{nm}$. The measured response time [rise, decay] is [10.3ms, 10.7ms] at room temperature. As the temperature decreases to -20°C , the decay time increases to 42ms. If we use a thinner cell gap (e.g. $d = 3\mu\text{m}$), the expected decay time, which is proportional to d^2 , is $\sim 30\text{ms}$. This result is $>10\text{X}$ faster than that of the MVA cell reported in Ref [4] at the same temperature. More details about the electro-optic properties using ultra-low viscosity and low dielectric anisotropy materials have been reported in Ref [15].

4. Discussion

Table 2 summarizes the measured physical properties of the five mixtures we prepared. Their Δn is around 0.1 and clearing point $\approx 80^\circ\text{C}$, which is desirable for FFS LCD applications. As $\Delta\varepsilon$ decreases from 6.2 to 3.1, γ_1 decreases from 53 mPas to 41 mPas. The correlation seems to be linear between these two parameters. To further investigate this empirical relation, more mixtures using the compounds listed in Table 1 are prepared for comparison. Figure 3 depicts the results, from which a linear relation between $\Delta\varepsilon$ and γ_1 is indeed observed. The extrapolated γ_1 is about 30 mPas for the employed non-polar diluters whose $\Delta\varepsilon \approx 0$. For some LCDs, such as desktop computers and TVs, they can afford to have a higher operation voltage, say 7.5V. Thus, we can use a lower $\Delta\varepsilon$ LC mixture and achieve a faster response time.

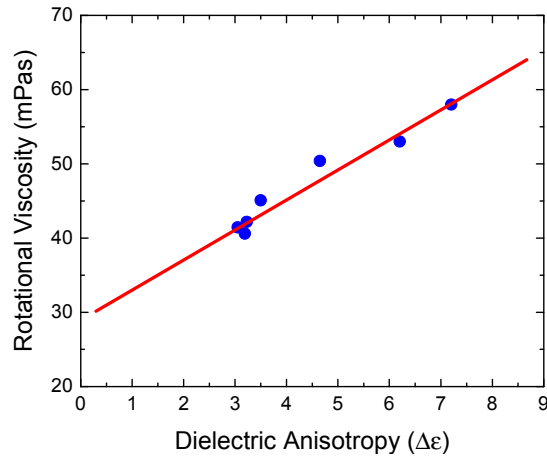


Fig. 3. Relation between rotational viscosity and dielectric anisotropy at 23°C .

5. Conclusion

We have formulated five ultra-low viscosity LC mixtures with positive $\Delta\varepsilon$ and characterized their physical properties. In addition to low viscosity, their Δn is around 0.1 and $T_c \sim 80^\circ\text{C}$, which is ideal for FFS LCDs. Another big advantage is their small activation energy, which significantly suppresses the rising rate of viscosity at low temperatures. Widespread applications of these ultra-low viscosity LC mixtures are expected.

Acknowledgment

The authors are indebted to AFOSR for partial financial supports under contract No. FA9550-14-1-0279.